Indian Journal of Engineering & Materials Sciences
Vol. 15, April 2008, pp. 147-151

Impedance analysis of $(Na_{0.5}Bi_{0.5})(Zr_{0.25}Ti_{0.75})O_3$ ceramic

Lily[a], K Kumari[a], K Prasad[a,*] & R N P Choudhary[b]

[a]University Department of Physics, T M Bhagalpur University, Bhagalpur 812 007, India
[b]Department of Physics and Meteorology, Indian Institute of Technology, Kharagpur 721 302, India

Received 2 November 2006; accepted 28 February 2008

$(Na_{0.5}Bi_{0.5})(Zr_{0.25}Ti_{0.75})O_3$, having perovskite-type orthorhombic structure, is prepared using via high-temperature solid-state reaction technique. The electrical behaviour has been assessed by electric modulus, pseudo Cole-Cole, and ac conductivity analyses. Electric modulus and pseudo Cole-Cole analyses indicated the dielectric relaxation to be of non-Debye type. The electrical conductivity studies showed the negative temperature coefficient of resistance character of $(Na_{0.5}Bi_{0.5})(Zr_{0.25}Ti_{0.75})O_3$. The ac conductivity is found to obey the universal power law and correlated barrier hopping model is found to successfully explain the electrical conduction in the system.

Keywords: $(Na_{0.5}Bi_{0.5})(Zr_{0.25}Ti_{0.75})O_3$, Impedance spectroscopy, Dielectric relaxation, Conductivity.

In recent years, there is a growing need of lead-free and/or low lead compositions for piezoelectric and pyroelectric applications. Sodium bismuth titanate, $(Na_{0.5}Bi_{0.5})TiO_3$ (NBT) is considered to be an excellent candidate as a key material of lead-free piezoelectric ceramic, which shows strong ferroelectric properties[1-7]. NBT belongs to perovskite family (ABO_3-type) with rhombohedral symmetry at ambient temperature. The A-site cations are considered to be ordered and the ferroelectric phase transition is found to be diffused one. During the past few years, a number of NBT based solid solutions have been tried to improve the electrical properties for their possible applications in electronic devices[8-15]. All these attempts have been made to modify the A-site, i.e., divalent pseudo-cation $(Na,Bi)^{2+}$. Further, it has been observed that modification at B-site plays an important role in tailoring electrical properties of perovskite systems[16-19]. An extensive literature survey suggested that no attempt, to our knowledge, has so far been made to study the Zr^{4+} modified $(Na_{0.5}Bi_{0.5})TiO_3$ ceramic. Considering above facts, the present work is an attempt to study the electrical properties (dielectric, electric modulus and ac conductivity) of $(Na_{0.5}Bi_{0.5})(Zr_{0.25}Ti_{0.75})O_3$ (abbreviated as NBZT) ceramic prepared through solid-state reaction method. Pseudo Cole-Cole analysis has been made to understand the dielectric relaxation in NBZT system.

*Forcorrespondence (E-mail: k_prasad65@yahoo.co.in)

Experimental Procedure

A high temperature solid-state reaction method was used to prepare $(Na_{0.5}Bi_{0.5})(Zr_{0.25}Ti_{0.75})O_3$ (NBZT) ceramic. To synthesize the NBZT samples, AR grade (99.9%+ pure) chemicals (Na_2CO_3, Bi_2O_3, ZrO_2 and TiO_2) were taken in stoichiometric ratios. The reactants were mixed thoroughly, using agate mortar and pestle in methanol medium. The mixture was pre-sintered at 1070°C for 4 h. Requisite amount of polyvinyl alcohol was added as a binder before making the pellets. Circular disc shaped pellet having geometrical dimensions: thickness = 2.81 mm and diameter = 10 mm was made to applying uniaxial stress of 6 MPa. The pellets were subsequently heated up to 1100°C for 3 h. Completion of the reaction and the formation of the desired compound were checked by X-ray diffraction technique. The XRD spectra were taken on calcined powders of NBZT with a X-ray diffractometer (Rikagu Miniflex, Japan) at room temperature using CuK_α radiation (λ = 0.15418 nm) over a wide range of Bragg angles ($20° \le 2\theta \le 80°$) with a scanning speed 2° min^{-1}. The electrical measurements were carried out on a symmetrical cell of type Ag|NBZT|Ag, where Ag is a conductive paint coated on either side of the pellet. Electrical impedance (Z), phase angle (θ), loss tangent ($\tan\delta$) and capacitance (C) were measured as a function of frequency (0.1 kHz-1 MHz) at different temperatures (30°C-500°C) using a computer-controlled LCR Hi-Tester (HIOKI 3532-50), Japan.

Results and Discussion

Figure 1 shows the X-ray diffraction pattern of NBZT at room temperature. A standard computer program (POWD) has been utilized for the XRD analysis. Good agreement between the observed and calculated inter-planer spacing (*d*-values) and no trace of any extra peaks due to constituent oxides, were found, suggesting the formation of a single-phase compound having orthorhombic structure.

The lattice parameters were found to be: a = 4.141(5) Å, b = 9.738(1) Å and c = 5.547(2) Å with an estimated error of $\pm 10^{-3}$Å. The volume of the unit cell was estimated to be 223.72 Å^3.

Figures 2 and 3 respectively, show the frequency dependence of real (ε') and imaginary (ε'') parts of dielectric constant at several temperatures.

It is observed that both ε' as well as ε'' in general follow inverse dependence on frequency, normally followed by almost all dielectric/ferroelectric materials except for ε'' at 400°C and 500°C. A dispersion with relatively high dielectric constant can be seen in the ε'-f graph in the lower frequency region and the dielectric constant drops at high frequencies. This is due to the fact that dipoles can no longer follow the field at high frequencies.

Inset Fig. 4 shows the variation of ε' and ε'' with temperature at 1 kHz and 10 kHz. It is observed that the values of ε' increase with temperature while ε'' finds a maxima.

The relaxation effects exhibited by NBZT have been analyzed by pseudo Cole-Cole plot method (instead of conventional Cole-Cole plot between $\varepsilon'(\omega)$ and $\varepsilon''(\omega)$ at fixed temperature) suggested by

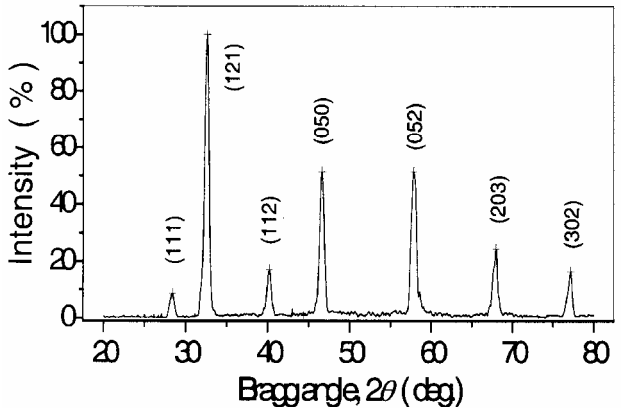

Fig. 1—X-ray diffraction pattern of NBZT at room temperature

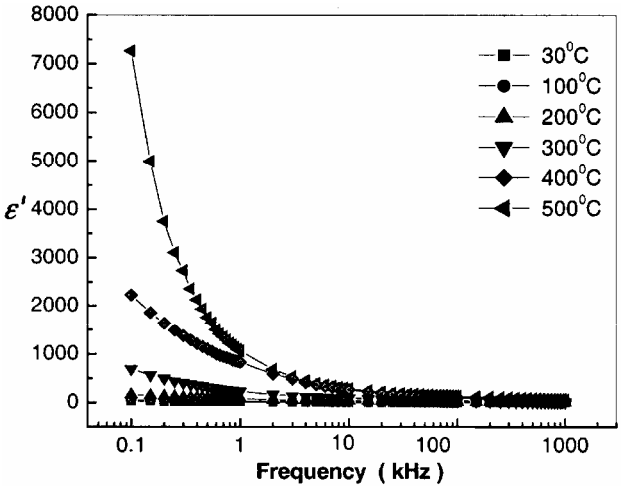

Fig. 2—Frequency dependence of real part dielectric constant of NBZT at different temperatures.

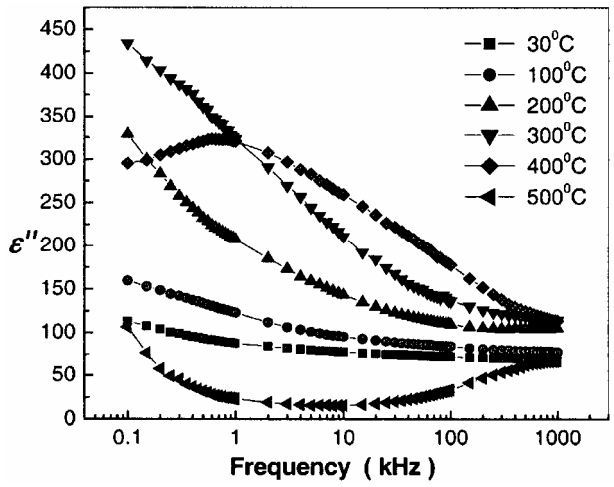

Fig. 3—Frequency dependence of imaginary part dielectric constant of NBZT at different temperatures.

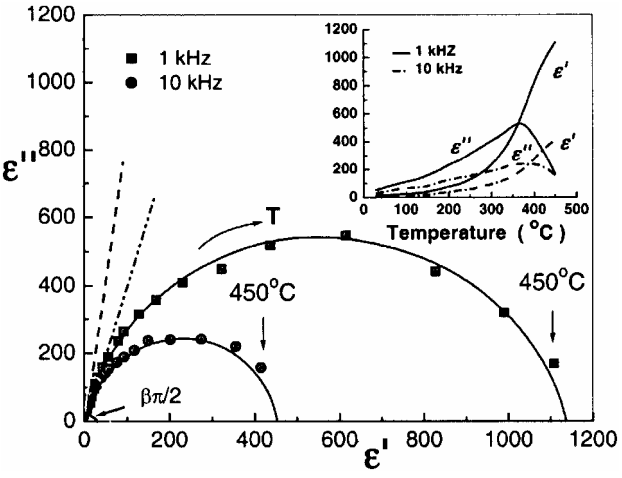

Fig. 4—Pseudo Cole-Cole plot of NBZT at 1 kHz and 10 kHz. Inset shows the variation of ε′ and ε′′ with temperature

Sixou *et al.*[20] where $\varepsilon'(\omega)$ versus $\varepsilon''(\omega)$ are plotted at a fixed frequency. Figure 4 shows the pseudo Cole-Cole plots at 1 kHz and 10 kHz. The nature of these plots indicates that the Cole-Davidson equation:

$$\varepsilon^*(\omega,T) = \varepsilon_\infty + \frac{\Delta\varepsilon}{(1+i\omega\tau)^\beta} \quad \ldots (1)$$

can safely be applied to this system. Here τ (= $1/2\pi f$) is the relaxation time, $\Delta\varepsilon$ $(= \varepsilon_s - \varepsilon_\infty)$ is the relaxation strength and β represents the magnitude of the departure of the electrical response from an ideal condition. When $\beta \rightarrow 1$, Eq.(1) gives rise to classical Debye's formalism. Separating real and imaginary parts of Eq.(1) and rewriting with explicit temperature dependence terms:

$$\varepsilon'(\omega,T) = \varepsilon_\infty + (\varepsilon_s - \varepsilon_\infty)\{\cos\phi(T)\}^\beta \cos\{\beta\phi(T)\} \quad \ldots (2)$$

$$\varepsilon''(\omega,T) = (\varepsilon_s - \varepsilon_\infty)\{\cos\phi(T)\}^\beta \sin\{\beta\phi(T)\} \quad \ldots (3)$$

where $\phi(T) = \tan^{-1}(\omega\tau)$. The plot between $\varepsilon'(\omega)$ and $\varepsilon''(\omega)$ given by Eqs (2) and (3) at fixed frequency is often called as pseudo Cole-Cole plot, which cuts ε'-axis at ε_s and ε_∞. Here, ε_s is high temperature dielectric constant (in contrast to the low frequency dielectric constant in the conventional Cole-Cole plot) and similarly ε_∞ is the low temperature dielectric constant. The plot cuts ε'-axis at low temperature side at an angle of $\beta\pi/2$. The value of $\Delta\varepsilon$ was estimated respectively to be 1134 and 449 at 1 kHz and 10 kHz. Also, the value of β comes to be 0.90 (for 1 kHz) and 0.81 (for 10 kHz), which indicates the dielectric relaxation in NBZT to be non-Debye type. This may be due to the presence of distributed elements in the material-electrode system[21].

The dielectric response of a material can be expressed in terms of a reciprocal quantity $M^*(\omega) = 1/\varepsilon^*(\omega)$, known as electric modulus in which the electrode polarization artifacts are suppressed. Typical features of $M^*(\omega)$ include a broad, asymmetric peak in the imaginary part and a sigmoidal step in the real part. The similarity of these shapes to loss and storage of mechanical stress associated with relaxation processes is evident and has naturally led to similar interpretation. The real and imaginary parts of electric modulus were obtained from the impedance data in accordance with the relations:

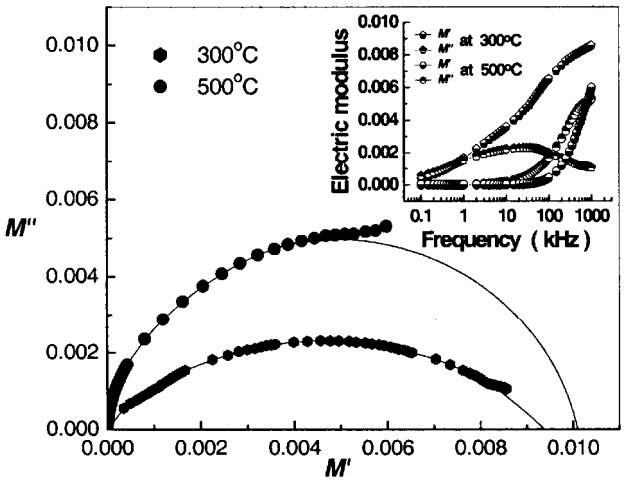

Fig. 5—Complex electric modulus plot of NBZT at 300°C and 500°C. Inset shows the variation of M' and M'' with frequency.

$$M' = \omega C_o Z'' \quad \ldots (4)$$

$$M'' = \omega C_o Z' \quad \ldots (5)$$

Figure 5 shows the complex electric modulus spectrum of NBZT at 300 and 500°C.

The patterns are characterized by the presence of little asymmetric and depressed semicircular arcs whose centre does not lie on M'-axis. The behaviour of electric modulus spectrum is suggestive of the temperature dependent hopping type of mechanism for electric conduction (charge transport) in the system[22] and non-Debye type dielectric relaxation. Inset Fig. 5 shows the variation of M' as well as M'' with frequency at two representative temperatures 300°C and 500°C. It is characterized by very low value (~zero) of M' in the low frequency region, a continuous dispersion with the increase in frequency having a tendency to saturate at a maximum asymptotic value designated as M_∞ in the high frequency region. Such observations may possibly be related to a lack of restoring force governing the mobility of charge carriers under the

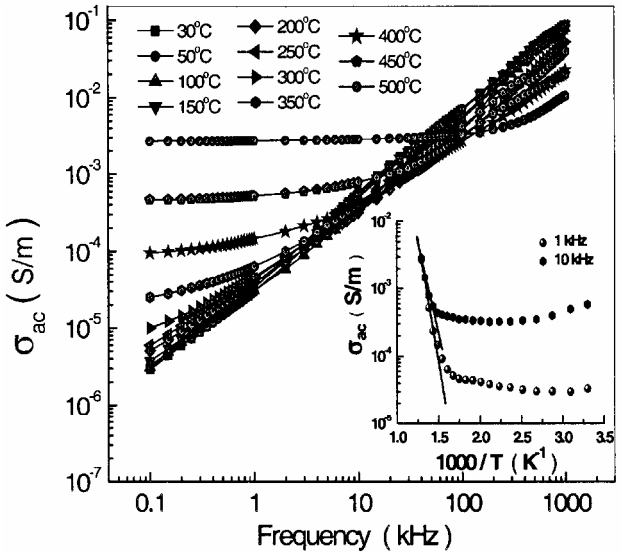

Fig. 6—Variation of ac conductivity with frequency at different temperatures for NBZT. Inset shows variation of ac conductivity with inverse of temperature at 1kHz and 10kHz.

action of an induced electric field. This behaviour supports long-range mobility of charge carriers. Further, a sigmoidal increase in the value of M' with the frequency approaching ultimately to M_∞, may be attributed to the conduction phenomena due to short-range mobility of charge carriers. The variation M'' as a function of frequency is characterized by: (i) clearly resolved peaks in the pattern appearing at unique frequency at different temperatures, (ii) significant asymmetry in the peak with their positions lying in the dispersion region of M' versus frequency pattern and (iii) the peak positions have a tendency to shift towards higher frequency side with the rise in temperature. The low frequency side of the M'' peak represents the range of frequencies in which charge carriers can move over a long distance, i.e., charge carriers can perform successful hopping from one site to the neighbouring site. The high frequency side of the M'' peak represents the range of frequencies in which the charge carriers are spatially confined to their potential wells and thus could be make localized motion within the well. The region where peak occurs is an indicative of the transition from long-range to short-range mobility with increase in frequency. Further, the appearance of peak in modulus spectrum provides a clear indication of conductivity relaxation[23]. Also, $M''(\omega)$ gets broadened upon increasing temperature suggesting an increase in non-Debye behaviour. This particular behaviour seems to be unique to electrical relaxation since all other relaxation processes (e.g. mechanical, light scattering) typically exhibit opposite behaviour with tendency towards Debye behaviour with increasing temperature[24].

The ac electrical conductivity was obtained using the relation:

$$\sigma_{ac} = l / SZ' \quad \ldots (6)$$

where l is the thickness and S is the surface area of the specimen. The variation of σ_{ac} of NBZT as a function of frequency at different temperatures is shown in Fig. 6. At low temperatures, σ_{ac} varies linearly with frequency. The frequency variation of σ_{ac} involves a power exponent ($\sigma_{ac} \propto \omega^n$, n is the exponent and can assume a value < 1 and ω is angular frequency of ac field). This indicates that the conduction process is a thermally activated process. From the graph it is seen that the exponent as depicted by the slope of the variation is a function of temperature. Further, the ac conductivity of the sample depends on its dielectric nature. At higher temperature, frequency independent ac conductivity is observed in low frequency region. This frequency independent region increases with increasing temperature and obeys the following phenomenological law[25]:

$$\sigma_{ac} = \sigma_{dc} + A.\omega^n \quad \ldots (7)$$

with $0 \le n \le 1$ and A is a thermally activated quantity and σ_{dc} the frequency independent (dc) part of conductivity. Also, it is observed that the electrical conductivity increases with the increase in temperature. A similar behaviour was observed in $(Na_{0.5}Bi_{0.5})ZrO_3$ ceramic[23]. We find the value of index n to decrease with the increasing temperature. The model based on classical hopping of electrons over barrier[26] predicts a decrease in the value of the index n with the increase in temperature and so found to be consistent with the experimental results. Thus, the hopping of electrons may be the dominating mechanism in the system. Inset Fig. 6 shows the variation of ac conductivity versus inverse of temperature at 1 kHz and 10 kHz.

The nature of variation is almost linear in the high temperature region obeys the Arrhenius relationship:

$$\sigma_{ac} = \sigma_o \exp(-E_a/k_BT) \quad \ldots (8)$$

where E_a is the activation energy of conduction and T is the absolute temperature. The nature of variation

shows the negative temperature coefficient of resistance (NTCR) behaviour of NBZT. The value E_a (= 1.061 eV at 1 kHz and 0.841 eV at 10 kHz) obtained by least squares fitting of the data at higher temperature region. It is observed that the value of E_a decreases with the increase in frequency. The low value of activation energy obtained could be attributed to the influence of electronic contribution to the conductivity. The increase in conductivity with temperature may be considered on the basis that within the bulk, the oxygen vacancies due to the loss of oxygen are usually created during sintering and the charge compensation follows the reaction (Kröger and Vink)[27]: $O_o \rightarrow \frac{1}{2}O_2 \uparrow + V_o^{\bullet\bullet} + 2e^-$, which may leave behind free electrons making them *n*-type[28].

Conclusions

Polycrystalline $(Na_{0.5}Bi_{0.5})(Zr_{0.25}Ti_{0.75})O_3$, prepared through a high-temperature solid-state reaction technique, was found to have a single-phase perovskite type orthorhombic structure. Electric modulus and pseudo Cole-Cole analyses indicated the dielectric relaxation to be of non-Debye type. The electrical conductivity studies showed the NTCR character of NBZT. The ac conductivity was found to obey the universal power law. The pair approximation type correlated barrier hopping (CBH) model successfully explained the universal behaviour of the exponent, *n*. Also, the frequency dependent ac conductivity at different temperatures indicated that the conduction process is thermally activated process.

Acknowledgement

One of us (KP) gratefully acknowledges Indian National Science Academy (INSA), New Delhi for providing visiting fellowship.

References

1 Buhrer C F, *J Chem Phys,* 36 (1962) 798.
2 Suchanicz J, Roleder K, Kania A & Handerek J, *Ferroelectrics,* 77 (1988) 107.
3 Roleder K, Suchanicz J & Kania A, *Ferroelectrics,* 89 (1989) 1.
4 Hosono Y, Harada K & Yamashita Y, *Jpn J Appl Phys*, 40 (2001) 5722.
5 Suchanicz J, Kusz J, Bhöm H, Duda H, Mercurio J P & Konieczny K, *J Eur Ceram Soc*, 23 (2003) 1559.
6 Gomah-Pettry J R, Saïd S, Marchet P & Mercurio J P, *J Eur Ceram Soc*, 24 (2004) 1165.
7 Xu Q, Chen S, Chen W, Wu S, Zhou J, Sun H & Li Y, *Mater Chem Phys*, 90 (2005) 111.
8 Lee J K, Hong K S, Kim C K & Park S E, *J Appl Phys,* 91 (2002) 4538.
9 Saïd S, Marchet P, Merle-Méjean T & Mercurio J P, *Mater Lett*, 58 (2004) 1405.
10 Saïd S & Mercurio J P, *J Eur Ceram Soc*, 21 (2001) 1333.
11 Saradhi B V B, Srinivas K & Bhimasankaram T, *Int J Mod Phys*, B 16 (2002) 1.
12 Li Y, Chen W, Zhou J, Xu Q, Sun H & Liao M, *Ceram Int*, 31 (2005) 139.
13 Yoo J, Oh D, Jeong Y, Hong J & Jung M, *Mater Lett*, 58 (2004) 3831.
14 Li Y, Chen W, Xu Q, Zhou J, Gu X & Fang S, *Mater Chem Phys*, 94 (2005) 328.
15 Li Y M, Chen W, Xu Q, Zhou J & Gu X, *Mater Lett*, 59 (2005) 1361.
16 Li Y M, Chen W, Zhou J, Xu Q, Gu X & Liao R H, *Physica B*: *Conden Mater*, 365 (2005) 76.
17 Li Y, Chen W, Zhou J, Xu Q, Sun H & Xu R, *Mater Sci Eng*, B 112 (2004) 5.
18 Wada T, Toyoike K, Imanaka Y & Matsuo Y, *Jpn J Appl Phys*, 40 (2001) 5703.
19 Ishii H, Nagata H & Takenaka T, *Jpn J Appl Phys*, 40 (2001) 5660.
20 Sixou P, Dansas P & Gillot D, *J Chim Phys*, 64 (1967) 834.
21 Macdonald J R, Ed, *Impedance Spectroscopy: Emphasizing Solid Materials and Systems* (John Wiley and Sons, New York), 1987.
22 Chandra K P, Prasad K & Gupta R N, *Physica B*: *Conden Mater*, 388 (2007) 118.
23 Lily, Kumari K, Prasad K & Yadav K L, *J Mater Sci*, 42 (2007) 6252.
24 Angell C A, *Chem Rev*, 90 (1990) 523.
25 Jonscher K, *Nature*, 267 (1977) 673.
26 Elliott S R, *Philos Mag B*, 37 (1978) 553.
27 Kröger F A & Vink H J, *Solid State Phys*, 3 (1956) 307.
28 Prasad K, Suman C K & Choudhary R N P, *Ferroelectrics*, 324 (2005) 89.